© 2025 Journal of Pharmacy & Pharmacognosy Research, 13 (3), 801-815, 2025
ISSN 0719-4250
https://jppres.com

DOI: https://doi.org/10.56499/jppres24.2049_13.3.801

Original Article

Hydroxyapatite, polyetheretherketone, and stainless steel as orthodontic mini-implant biomaterial candidates: A bioinformatic approach

[Hidroxiapatita, polieteretercetona y acero inoxidable como candidatos a biomateriales para mini-implantes de ortodoncia: Un enfoque bioinformático]

I Gusti Aju Wahju Ardani[1*], Mario Raphael Sugitto[1], Hashfi Raushan Aufa[1], Viol Dhea Kharisma[2], Ananda Firman Putranto[1], Guruh Putra Gunung[1], Ida Bagus Agastya Perkasa[1], Achmad Syaifudin[3], Putri Cahaya Situmorang[4], Rozita Hassan[5], Alexander Patera Nugraha[1]

[1]Orthodontic Department, Faculty of Dental Medicine, Universitas Airlangga, Surabaya, 60132, East Java, Indonesia.
[2]Doctoral Student of Biology, Faculty of Science and Technology, Universitas Airlangga, Surabaya.
[3]Department of Medical Technology, Faculty of Medicine and Health, Institut Teknologi Sepuluh November, Surabaya, East Java, Indonesia.
[4]Study Program of Biology, Faculty of Mathematic and Natural Science, Universitas Sumatera Utara, Medan, Indonesia.
[5]Orthodontic Unit, Faculty of Dentistry, Universiti Sains Malaysia, Kota Bahru, Kelantan, Malaysia.
*E-mail: wahju_ardani@fkg.unair.ac.id

Abstract

Context: Orthodontic mini-implants (OMIs) are temporary devices affixed to bones that aim to improve absolute anchoring during orthodontic treatment for malocclusion. Stainless steel (SS), polyetheretherketone (PEEK), and hydroxyapatite (HA) are substitute materials that might work well together. To determine how SS, PEEK, and HA interact with bone molecular target proteins linked to resistant types of OMI, a molecular docking investigation and an *in silico* analysis were carried out.

Aims: To analyze the binding activity of SS, PEEK, and HA to bone molecular target proteins *in silico* as potential OMI biomaterial candidates.

Methods: Osteocalcin, osteonectin, bone morphogenic protein (BMP)4, BMP2, BMP7, alkaline phosphatase (ALP), runt-related transcription factor-2 (RUNX2), insulin growth factor-1 (IGF1), osterix, tartrate-resistant acid phosphatase (TRAPase), and collagen type 1a1 (COL1A1) biomolecular interaction patterns were used in molecular docking to identify ligand activity on target proteins using negative binding affinity. Network prediction was used to investigate the activation and inhibition of the ligand complex on target proteins.

Results: Bone molecular target proteins, such as IGF1 and osteopontin, bind to SS, PEEK, and HA ligands with a strong negative binding affinity, causing ligand activation or inhibition. Out of all the variables, the combination of SS, PEEK, and HA had the largest negative value.

Conclusions: As shown *in silico*, SS, PEEK, and HA ligands have a high binding affinity for resistance-form-related bone target proteins, such as IGF1 and osteopontin, making them potentially useful as OMI biomaterials.

Keywords: hydroxyapatite; medicine; orthodontic mini-implant; polyetheretherketone; resistance for; stainless steel.

Resumen

Contexto: Los mini-implantes de ortodoncia (OMI) son dispositivos temporales que se fijan a los huesos y que tienen como objetivo mejorar el anclaje absoluto durante el tratamiento de ortodoncia para la maloclusión. El acero inoxidable (SS), la polieteretercetona (PEEK) y la hidroxiapatita (HA) son materiales sustitutos que podrían funcionar bien juntos. Para determinar cómo interactúan SS, PEEK y HA con las proteínas moleculares óseas dianas vinculadas a los tipos resistentes de OMI, se llevó a cabo una investigación de acoplamiento molecular y un análisis *in silico*.

Objetivos: Analizar la actividad de unión de SS, PEEK y HA a las proteínas moleculares óseas diana *in silico* como posibles candidatos a biomateriales OMI.

Métodos: Se utilizaron patrones de interacción biomolecular de osteocalcina, osteonectina, proteína morfogénica ósea (BMP)4, BMP2, BMP7, fosfatasa alcalina (ALP), factor de transcripción relacionado con runt-2 (RUNX2), factor de crecimiento de insulina-1 (IGF1), osterix, fosfatasa ácida resistente al tartrato (TRAPasa) y colágeno tipo 1a1 (COL1A1) en el acoplamiento molecular para identificar la actividad del ligando en proteínas objetivo utilizando afinidad de unión negativa. Se utilizó la predicción de red para investigar la activación e inhibición del complejo de ligando en proteínas objetivo.

Resultados: Las proteínas objetivo-moleculares óseas, como IGF1 y osteopontina, se unen a los ligandos SS, PEEK y HA con una fuerte afinidad de unión negativa, lo que provoca la activación o inhibición del ligando. De todas las variables, la combinación de SS, PEEK y HA tuvo el valor negativo más grande.

Conclusiones: Como se muestra *in silico*, los ligandos SS, PEEK y HA tienen una alta afinidad de unión por las proteínas óseas dianas relacionadas con la forma de resistencia, como IGF1 y osteopontina, lo que los hace potencialmente útiles como biomateriales OMI.

Palabras Clave: acero inoxidable; hidroxiapatita; medicina; mini-implante de ortodoncia; polieteretercetona; resistencia para.

ARTICLE INFO
Received: April 10, 2024.
Accepted: November 29, 2024.
Available Online: December 24, 2024.

AUTHOR INFO
ORCID:
0000-0002-4874-2906 (IGAWA)
0000-0001-9060-0429 (VDK)
0000-0002-0960-8739 (AFP)
0000-0001-8109-9396 (AS)
0000-0002-9895-1853 (PCS)
0000-0002-3088-2169 (RH)
0000-0001-7427-7561 (APN)

Abbreviations: ADMET: absorption–distribution–metabolism–excretion–toxicity; ALP: alkaline phosphatase; BIC: bone implant contact; BMP: bone morphogenic protein; CID: compound identifier; COL1: type I collagen; COL1A1: collagen type 1a1; HA: hydroxyapatite; IGF1: insulin growth factor-1; OMIs: orthodontic mini-implants; PDB: protein databank; PEEK: polyetheretherketone; RCSBPDB: Research Collaboratory for Structural Bioinformatics Protein Data Bank; RUNX2: runt-related transcription factor-2; SDF: structure data format; SID: substance identifier; SMILE: simplified molecular input line entry system; SS: stainless steel; TADs: temporary anchoring devices; TRAPase: tartrate-resistant acid phosphatase.

INTRODUCTION

The third most prevalent oral health issue worldwide is malocclusion. About 80% of people in Indonesia have it, and it comes in third place behind periodontal disease and dental caries (Ardani et al., 2020). A mismatch in the connection between the upper and lower jaws or a misalignment of the teeth are characteristics of malocclusion, an aberrant occlusion (Putri et al., 2024). In the realm of health, particularly in the field of orthodontics, the severity of malocclusion and its impact on oral function and appearance must be a priority (Syahdinda et al., 2022). Two categories of causes contribute to malocclusion: general factors and local ones. Concerns that do not directly impact the teeth are referred to as general issues. According to Putri et al. (2024), local variables are those that have an immediate impact on the malocclusion.

A patient's quality of life may be negatively impacted by malocclusion if they have trouble speaking, biting, or chewing as well as cleaning their teeth, or are more likely to develop cavities and periodontal disease. Orthodontic techniques are used to treat malocclusion and return the occlusion to its optimal condition (Alhammadi et al., 2023). To enhance masticatory, phonetic, and cosmetic functions, orthodontic treatment is used to correct bite overlaps and spacing, align teeth, and remove occlusion damage (Gkantidis et al., 2010). Orthodontists use appliances to shift teeth as necessary during orthodontic treatment to address patients' issues (Leo et al., 2016). Anchorage is one of the key elements of orthodontic treatment. To stop anchoring teeth from being lost, absolute anchorage is required. Only dental orthodontic mini-implants (OMIs) can provide complete anchoring (Park et al., 2021). To increase success rates and clinical performance, new materials for temporary anchoring devices (TADs) or OMIs must be discovered. Improved bioactivity is another benefit of developing novel materials, and bone molecular interaction may enhance OMI's stability and performance, resulting in a more resistant form of OMIs with the surrounding alveolar bone tissue (Byeon et al., 2022). OMIs are TADs inserted into the bone to strengthen anchoring or lower the requirement for anchorage units. Because the reciprocal stresses from anterior retraction are transferred to the alveolar bone without engaging the posterior teeth and are unaffected by patient compliance, OMIs are thought to be able to provide absolute anchoring (Ardani et al., 2023).

Because of their superior mechanical qualities over alternative materials, metals are frequently utilized in biomaterial applications in the orthopedic and dentistry domains. Metals are often utilized as orthopedic and dental implants because of their many benefits over other materials, including tensile strength, youthful modulus, toughness, corrosion resistance, malleability, and simplicity of engineering (Ardani et al., 2024). Because of its excellent mechanical qualities and resistance to corrosion, stainless steel (SS) is a metal that is frequently utilized for OMIs. However, because metal materials emit metal ions, they can potentially trigger allergic responses when applied to the oral cavity (Berniyanti et al., 2022).

Due to its biocompatibility with the human body, polyetheretherketone (PEEK) is a polymer that is frequently utilized as an implant base material. Because PEEK is a non-toxic biopolymer with an elastic modulus comparable to that of human bone, it is available as a mini-implant biomaterial. Furthermore, it is simpler to manufacture, has color stability, and provides superior stress shielding (Ma et al., 2020). The best material in this situation is hydroxyapatite (HA), which shares structural and functional similarities to the mineral composition of bone and teeth. Materials that are compatible with human bone tissue and can prevent immune system rejection reactions can, therefore, be added to improve implant attachment to bone (Neto et al., 2023; Saskianti et al., 2022). According to one research (Cheng et al., 2012), a thin nano-HA coating applied electrochemically to ovariectomized rats' implants may improve osseointegration. Nano-HA is a powder composed of nanosized HA particles. Nano-HA particles have high crystallinity and are nanorod in shape. Typically, HA particles are ground into a fine powder to form nano-HA. Known for its biocompatibility, nano-HA is used in toothpaste, dental implants, and bone grafts, among other medical and dental applications (Byeon et al., 2022; Makar et al., 2023).

Enhancing OMIs' resistance form is mostly dependent on bone molecular protein interaction. OMIs' stability refers to the biological stability between bone remodeling and regeneration, whereas primary stability is associated with the implant's mechanical attachment to the cortical bone. The success of an implant depends on its lack of mobility and ability to swell the implant-bone interface before loading. To

increase bone molecular interaction and, in turn, form resistance in OMIs, a variety of techniques, including surface modification and material improvement, have been investigated (Alenezi et al., 2019; Byeon et al., 2022; Kayhan and Kazazoğlu., 2018). It is anticipated that the outstanding qualities of SS, PEEK, and nano-HA material combinations will enhance one another. These material combinations are expected to possess the bone regeneration capacity required for anchoring and thus be utilized as OMI biomaterials. However, there has been little research into combining SS, PEEK, and nano-HA as an OMI material. To determine how SS, PEEK, and nano-HA interact with target proteins in bone involved in regeneration, this study will use molecular docking to examine biomaterial combinations.

MATERIAL AND METHODS

Ligand retrieval

The ligands used in this study were PEEK, nano-HA, and SS. The ligand information consists of the following: name, symbol, formula, compound identifier (CID), simplified molecular input line entry system (SMILE), molecular weight, link, and structure data format (SDF) file. PubChem (https://pubchem.ncbi.nlm.nih.gov/) is a database that stores different types of information, including biological activity of compounds and substances, natural and synthetic chemical compounds, and biological activity of compounds and substances. It includes tools for drawing target compounds, a periodic table of elements, and query similarity identification (Kharisma et al., 2021a; Kim, 2016).

Energy minimization

Docking simulations reveal that the chemical interactions in the ligand SDF files retrieved from the PubChem database are inflexible. OpenBabel v2.3.1 software was used to convert the SDF file into protein databank (PDB) format on the query ligand. When engaging with the target domain, this procedure seeks to make the ligand's molecular interactions more flexible (Kharisma et al., 2020; Listiyani et al., 2022; Prahasanti et al., 2021).

Protein preparation

Alkaline phosphate (ALP), runt-related transcription factor-2 (RUNX2), insulin growth factor-1 (IGF1), osterix, osteopontin, osteocalcin, osteonectin, bone morphogenic protein (BMP)2, BMP4, BMP7, tartrate-resistant acid phosphatase (TRAPase), and collagen type 1a1 (COL1A1) were among the targets used in this study. They were sourced from the Research Collaboratory for Structural Bioinformatics Protein Data Bank (RCSBPDB) database (https://www.rcsb.org/). The target data retrieved from the RCSBPDB include the following: name, PDB ID, chain, sequence length, weight (kDa), resolution, visualization technique, and PDB file. The RCSB PDB is a structural database that contains data on proteins from wet lab studies, including both wild-type and mutant proteins (Ramadhani et al., 2022; Rose et al., 2017).

Target purification

Both natural ligands and water molecules present in the targets retrieved from the RCSB PDB database have the potential to disrupt the stability of ligand-protein interactions and the development of binding affinity during docking simulations. PyMol v2.5.2 software (Schrödinger, Inc., USA) with an academic license was used to remove native ligands and water molecules from the targets (Tošović et al., 2022).

Molecular docking simulation

Molecular docking is a method that determines ligand activity on the target proteins by analyzing patterns of molecular interactions and binding affinity. The docking grid, consisting of the X, Y, and Z axes in the center and dimensions, directs the ligand to the target domain (Ivanova and Karelson, 2022; Nugraha et al., 2023). To evaluate ligand activity, the grid type used in this study was a screening type that ignored the active side's position on the target proteins (Karakoti et al., 2022). Docking simulations with target proteins, such as osteopontin, osteocalcin, osteonectin, BMP4, BMP2, BMP7, ALP, RUNX2, IGF1, osterix, TRAPase, and COL1A1, were carried out on SS and nano-HA nanoparticles using the PyRx v1.0.0 software (Scripps Research, USA) with an academic license.

Molecular visualization

The ligand-protein molecular complex's three-dimensional structure was shown using PyMol v2.5.2 software (Schrödinger, Inc., USA), which was licensed for academic use. Sticks, cartoons, and translucent surfaces were used in a structural selection approach for visualization. To provide a single hue and representative look per publishing requirements, the staining selection was carried out on target proteins based on representation (García-Ortegón et al., 2022; Kharisma et al., 2021b).

Network prediction

The purpose of network prediction in this work was to identify the process by which ligand complexes on target proteins were activated and inhibited. Cytoscape v3.9.1 software was used to identify the network, which had a route confidence value of 0.40

in the human body and a maximum interactor of 15–25. The T-shapes and arrows show the ligand action on the target proteins (Cecilia et al., 2024; Daina et al., 2019; Mousavian et al., 2021).

Data analysis

Biomaterials consisting of PEEK, nano-HA, and SS with SDF files were obtained from PubChem. Absorption–distribution–metabolism–excretion–toxicity (ADMET) prediction was not performed in this study since the ligand was a biomaterial consisting of substances and nanoparticles rather than a compound (Bueno, 2020; Yusuf et al., 2023). Docking was performed using a variety of ligand combinations, including SS (as reference or golden standard), SS + HA, SS + PEEK + HA, HA, and PEEK, with twelve target proteins, obtained grid position data (center and dimension) and bond affinity values. Identification of chemical bond interaction and visualization of the three-dimensional structure of docking results were performed on ligand-protein complexes with the greatest negative binding affinity value. Determining the target protein pathway involved setting the confidence value to 0.40 (medium) and the interactor to 15–25 to predict the target's mechanism of action after binding to biomaterials (Mousavian et al., 2014). The server's analysis using the calculation model yielded predictions for the Lipinski rule, absorption, distribution, and toxicity. The prediction process started with the input of canonical SMILE data from each compound, followed by running the server and obtaining the predicted value. Based on the data acquired, the analysis yielded pathway images and assessment tables (Delicia et al., 2024).

RESULTS

The ligands utilized in this investigation as the reference were PEEK, nano-HA, and SS. The details gleaned from the PubChem database (https://pubchem.ncbi.nlm.nih.gov/) included the ligands' name, symbol, type, molecular weight (g/mol), formula, CID or substance identifier (SID), and two-dimensional structure in an SDF file (Table 1). The targets employed in this study were osteopontin, osteocalcin, osteonectin, BMP4, BMP2, BMP7, ALP, RUNX2, IGF1, osterix, TRAPase, and COL1A1. The RCSB PDB database (https://www.rcsb.org/) provided .pdb files containing information on each target, including name, ID, weight (kDa), chain type, visualization technique, resolution, sequence length, and three-dimensional structure in Fig. 1 and Table 2.

Table 1. Results of ligand preparation from PubChem.

Name	Symbol	Type	Molecular weight (g/mol)	Formula	CID/SID
Stainless steel	SS	Nanoparticle	55.84	Fe	23925
Hydroxyapatite	HA	Nanoparticle	502.3	$Ca_5HO_{13}P_3$	14781
Polyetheretherketone	PEEK	Substance	-	-	135076451

PubChem (https://pubchem.ncbi.nlm.nih.gov/)

Table 2. Results of protein target preparation from RCSB PDB.

No	Name	PDB ID	Weight (kDa)	Chain	Visualization method	Resolution	Sequence length
1	Osteopontin	1MOY	13.80	A	X-ray	1.55	130
2	Osteocalcin	1QSH	5.85	A	X-ray	2.00	49
3	Osteonectin	1BMO	55.23	A/B	X-ray	3.10	233
4	BMP4	1REU	11.73	A	X-ray	2.65	103
5	BMP2	4UI1	51.34	A/B	X-ray	2.35	114
6	BMP7	1LX5	29.23	A	X-ray	3.30	139
7	AP	2GLQ	53.57	A	X-ray	1.60	484
8	RUNX2	6VGE	62.53	D	X-ray	4.25	117
9	IGF1	1IGR	57.07	A	X-ray	2.60	478
10	Osterix	6X46	14.35	A	NMR	-	121
11	TRAPase	1WAR	35.48	A	X-ray	2.22	310
12	COL1A1	2LLP	4.97	A/B/C	NMR	-	18

RCSB PDB (https://www.rcsb.org/)

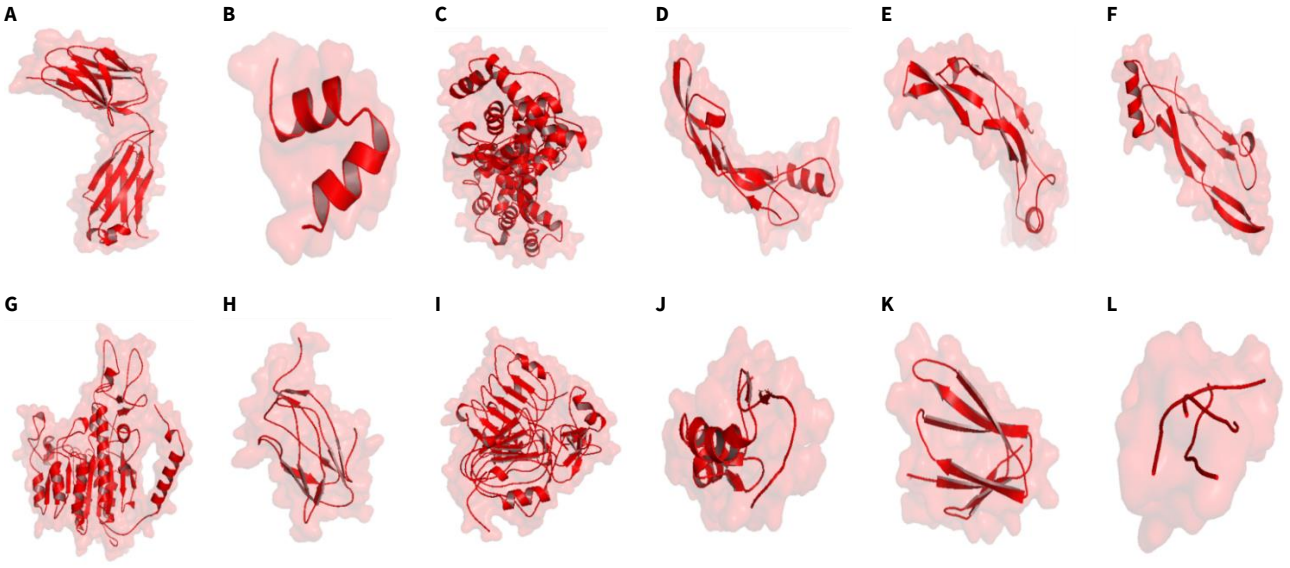

Figure 1. Three-dimensional structure.
(A) Osteopontin; **(B)** Osteocalcin; **(C)** Osteonectin; (**D**) BMP4; **(E)** BMP2; **(F)** BMP7; **(G)** ALP; **(H)** RUNX2; **(I)** IGF1; **(J)** Osterix; **(K)** TRAPase; **(L)** COL1A1.

The targets osteopontin, osteocalcin, osteonectin, BMP4, BMP2, BMP7, ALP, RUNX2, IGF1, osterix, and COL1A1 may all bind to the SS + PEEK + HA complex, resulting in enhanced target activity and TRAPase inhibition (Table 3). Using transparent-rigid surfaces and cartoons with a single coloring method for the target and based on C, H, O, and N atoms for the ligand, the three-dimensional structure of the docking results was shown using PyMol v2.5.2 (Schrödinger, Inc., USA) under an academic license (Fig. 2). The molecular interaction analysis found that the SS-HA-PEEK ligand complex functioned as a TRAPase inhibitor through weak connections made up of hydrogen, van der Waals, and pi/alkyl bonds (Table 4), rather than forming unfavorable interactions with all targets (Fig. 3). Due to >0 and <2 scores, the SS-HA-PEEK route can initiate target actions such as activation and inhibition upon binding to all targets, in terms of the average number of neighbors and typical path length (Table 5). After obtaining the protein route from the Cytoscape database, the target interacted with the SS-HA-PEEK ligand combination (Fig. 4).

DISCUSSION

The objective of this study was to ascertain the *in silico* analysis of OMI biomaterials based on SS, PEEK, and nano-HA on bone biomarkers related to enhanced bone molecular interaction-induced resistant forms of OMI. To be used as OMI biomaterials, these material combinations must have the requisite bone contact ability to induce resistant forms of OMI and perform absolute anchorage. Bone implant contact (BIC) is the biological fixation of an implant that is in direct bone contact with the implant without the intervention of connective tissue; this bone contact is regarded as a crucial indicator of successful OMI absolute anchorage and an important sign of a good resistant form of OMI (Ardani et al., 2024). Numerous elements impact OMI's resistance, including the implant's location in the body, size, and design, as well as surgical techniques, load effects, age, gender, and surface features, such as roughness, wettability, chemical composition, and amorphous and crystalline phases (Ardani et al., 2022).

In this study, a simulation of ligand interaction with the target was identified through a virtual screening method, which aimed to determine the ligand's binding ability to attach to the target domain. The level of interaction activity between the ligand and the target protein was identified with reference to the resulting binding affinity. Binding energy, also known as binding affinity, is generated when a ligand interacts with a specific function of the target protein (Botelho et al., 2020). High binding ability and ligand activity, such as inhibition or activation, are indicated by binding affinities with greater negative values (Ertan-Botelli and Bolelli, 2021; Shallangwa and Adeniji, 2021). Binding affinity is a reference for determining ligand binding activity to the target. The negative binding energy that forms in the ligand-protein complex is known as binding affinity. The energy follows Gibbs' law, which states that the stronger the bonding contact, the more stable the molecule complex (Hata et al., 2021).

Table 3. Results of molecular docking simulation.

Protein	AutoGrid		Binding affinity (kcal/mol)				
	Center (Å)	Dimensions (Å)	SS	SS + HA	SS + PEEK + HA	HA	PEEK
Osteopontin	X: -13.072 Y: 8.032 Z: -26.462	X: 49.106 Y: 45.855 Z: 90.835	-1.3	-5.4	-13.7	-4.4	-7.5
Osteocalcin	X: 8.075 Y: 25.301 Z: 22.863	X: 31.622 Y: 16.932 Z: 12.741	-1.0	-4.5	-9.6	-3.4	-5.0
Osteonectin	X: 38.336 Y: 17.717 Z: 19.753	X: 113.749 Y: 77.848 Z: 100.817	-1.6	-5.7	-13.5	-4.4	-8.0
BMP4	X: -18.049 Y: -21.889 Z: -40.967	X: 45.418 Y: 70.381 Z: 54.455	-1.1	-3.5	-12.0	-3.5	-7.5
BMP2	X: 21.772 Y: 9.258 Z: 9.272	X: 50.303 Y: 49.492 Z: 61.623	-1,0	-4,8	-11.7	-3.6	-7.4
BMP7	X: 79.198 Y: 35.787 Z: 45.641	X: 69.668 Y: 31.390 Z: 36.941	-1.1	-4.9	-11.9	-3.9	-7.1
AP	X: 43.874 Y: 23.207 Z: 9.206	X: 83.550 Y: 75.117 Z: 72.897	-1.2	-6.0	-13.6	-4.2	-8.7
RUNX2	X: -50.956 Y: 39.759 Z: -15.612	X: 64.939 Y: 22.064 Z: 47.175	-1.2	-5.5	-12.6	-4.2	-6.3
IGF1	X: 40.018 Y: 29.479 Z: 52.605	X: 69.831 Y: 104.505 Z: 77.752	-1.3	-6.0	-14.3	-4.6	-8.7
Osterix	X: 3.944 Y: 3.965 Z: -46.055	X: 85.318 Y: 40.505 Z: 44.847	-1.0	-4.7	-11.1	-3.7	-6.8
TRAPase	X: 68.142 Y: -24.322 Z: 17.856	X: 33.318 Y: 38.191 Z: 40.670	-1.1	-4.7	-11.3	-4.0	-6.7
COL1A1	X: 0.338 Y: 0.089 Z: -0.003	X: 61.634 Y: 21.594 Z: 25.695	-0.9	-4.0	-9.5	-3.6	-5.6

SS: Stainless steel; HA: Hydroxyapatite; PEEK: Polyetheretherketone.

The findings revealed that the ligands SS, PEEK, and HA had a greater negative binding affinity value for bone molecular biomarkers linked to the formation of OMI resistance. By binding to osteopontin, osteocalcin, BMP2, BMP4, BMP7, ALP, RUNX2, IGF1, osterix, COL1A1, and TRAPase targets, the SS + PEEK + HA complex initiated ligand functions, such as activation or inhibition. According to earlier studies (Prahasanti et al., 2021), the HA-PEEK combination may have an impact on target protein function. A larger chance of OMI manufacturing may also result from the combination of PEEK and HA, raising osteogenic markers. Target proteins linked to enhancing OMI resistance, including osteopontin, osteocalcin, osteonectin,

BMP4, BMP2, BMP7, ALP, RUNX2, IGF1, osterix, TRAPase, and COL1A1, were shown to have a greater binding affinity when PEEK and HA were combined. This implies that PEEK and HA together may enhance OMI stability by stimulating bone molecular markers (Ardani et al., 2022).

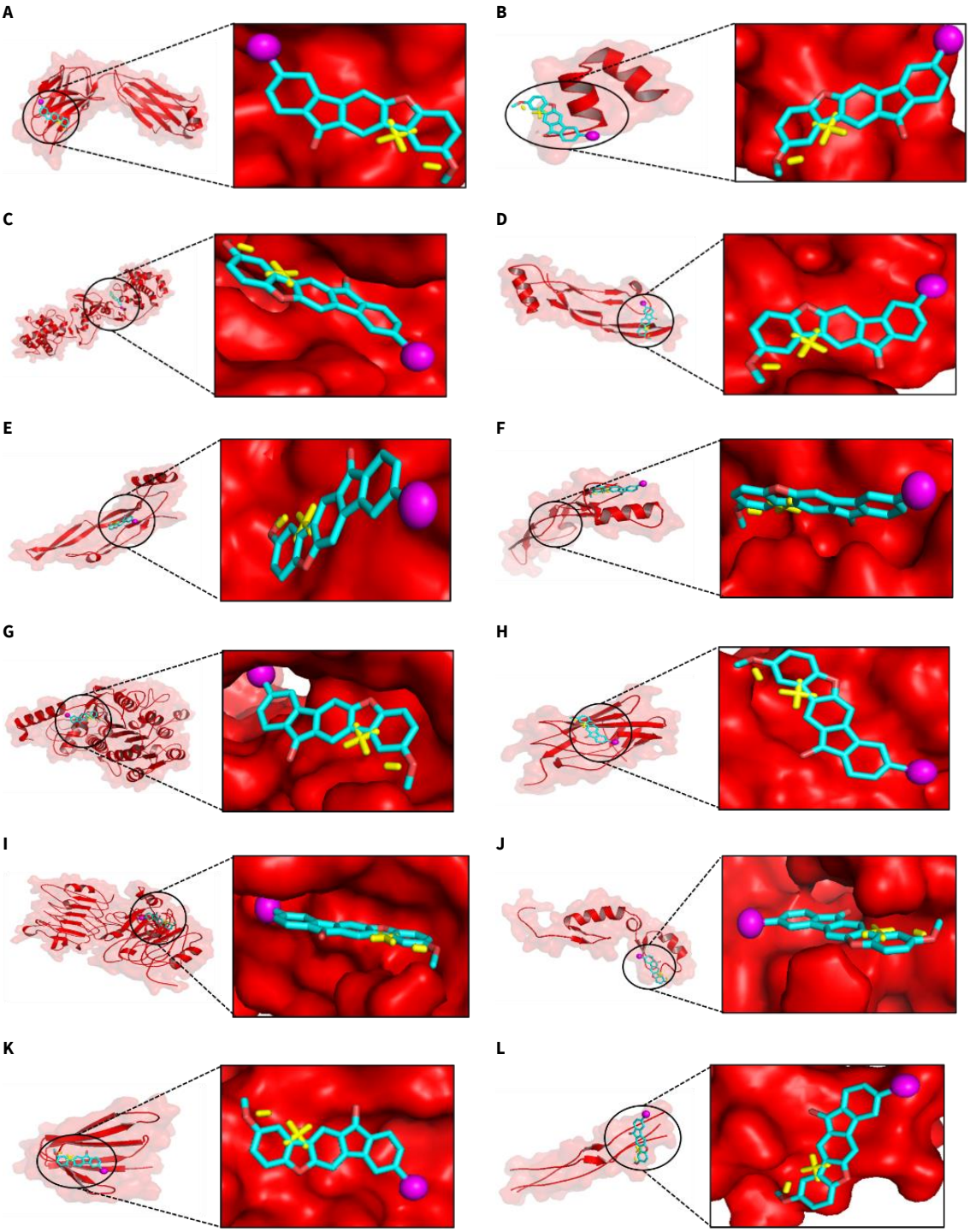

Figure 2. Structural visualization of ligand-target binding from the docking simulation, SS (purple), HA (yellow), PEEK (cyan), and the target domain (red).

(A) Osteopontin-SS-HA-PEEK; **(B)** Osteocalcin-SS-HA-PEEK; **(C)** Osteonectin-SS-HA-PEEK; **(D)** BMP4-SS-HA-PEEK; **(E)** BMP2-SS-HA-PEEK; **(F)** BMP7-SS-HA-PEEK; **(G)** ALP-SS-HA-PEEK; **(H)** RUNX2-SS-HA-PEEK; **(I)** IGF1-SS-HA-PEEK; **(J)** Osterix-SS-HA-PEEK; **(K)** TRAPase-SS-HA-PEEK; **(L)** COL1A1-SS-HA-PEEK.

Table 4. Protein-ligand interaction.

Protein-ligand	Chemical Interaction
Osteopontin-SS-HA-PEEK	van der Waals: - Hydrogen: - Pi/Alkyl: Phe91, Tyr49, Gln89
Osteocalcin-SS-HA-PEEK	van der Waals: Gln39, Tyr42, Tyr46, Gly47, Ile48 Hydrogen: - Pi/Alkyl: Arg43
Osteonectin-SS-HA-PEEK	van der Waals: - Hydrogen: Lys262, His232 Pi/Alkyl: His122, Lys123, His125
BMP4-SS-HA-PEEK	van der Waals: - Hydrogen: Tyr91, Asp93 Pi/Alkyl: Trp31, Trp28
BMP2-SS-HA-PEEK	van der Waals: - Hydrogen: Cys361, Val362, Pro363, Asp387 Pi/Alkyl: Ala322, His326
BMP7-SS-HA-PEEK	van der Waals: - Hydrogen: Leu75, Phe73 Pi/Alkyl: Ile86, Pro74, Leu90, Phe93
AP-SS-HA-PEEK	van der Waals: - Hydrogen: Glu347, Glu348 Pi/Alkyl: Ala29, Pro75, Ala22, Leu26
RUNX2-SS-HA-PEEK	van der Waals: - Hydrogen: Leu168, Ser165 Pi/Alkyl: Ala171, Met157
IGF1-SS-HA-PEEK	van der Waals: Leu384, Tyr391, Tyr388, Asp446, Ser443 Hydrogen: Asn478 Pi/Alkyl: Asn478, Tyr417
Osterix-SS-HA-PEEK	van der Waals: Gln58, Glu78, His67 Hydrogen: Arg56, Ser76 Pi/Alkyl: Asp80
TRAPase-SS-HA-PEEK	van der Waals: Ser72 Hydrogen: Glu73, Val57 Pi/Alkyl: Ile63, Ile70
COL1A1-SS-HA-PEEK	van der Waals: - Hydrogen: Val23, Gly25, Val24 Pi/Alkyl: Leu26, Pro27, Leu26

The goal of applying HA was to enhance the osteoconductive properties of HA coatings (Khotib et al., 2019; Naini et al., 2019). Applying HA to the implant surface can accelerate bone adaptation. The crystallinity and purity of HA are important for its efficacy as an implant surface coating, with a higher percentage of crystallinity positively correlating with lower biodegradation and resorbability (Levingstone et al., 2015). Nano-HA-coated implants improved osseointegration, resulting in favorable BIC as assessed by microtomographic and histomorphometric evaluation. Several variables affected implant osseointegration, and the success of implant therapy depended on factors such as bone volume, implant geometry, surface topography, patient systemic health, and local factors (Najeeb et al., 2016).

The molecular interactions in ligand-protein complexes are made up of multiple weak bond types at the target binding site. The binding site is the area where the ligand attaches to the target to influence particular biological processes, including activation or inhibition (Konc and Janežič, 2022).

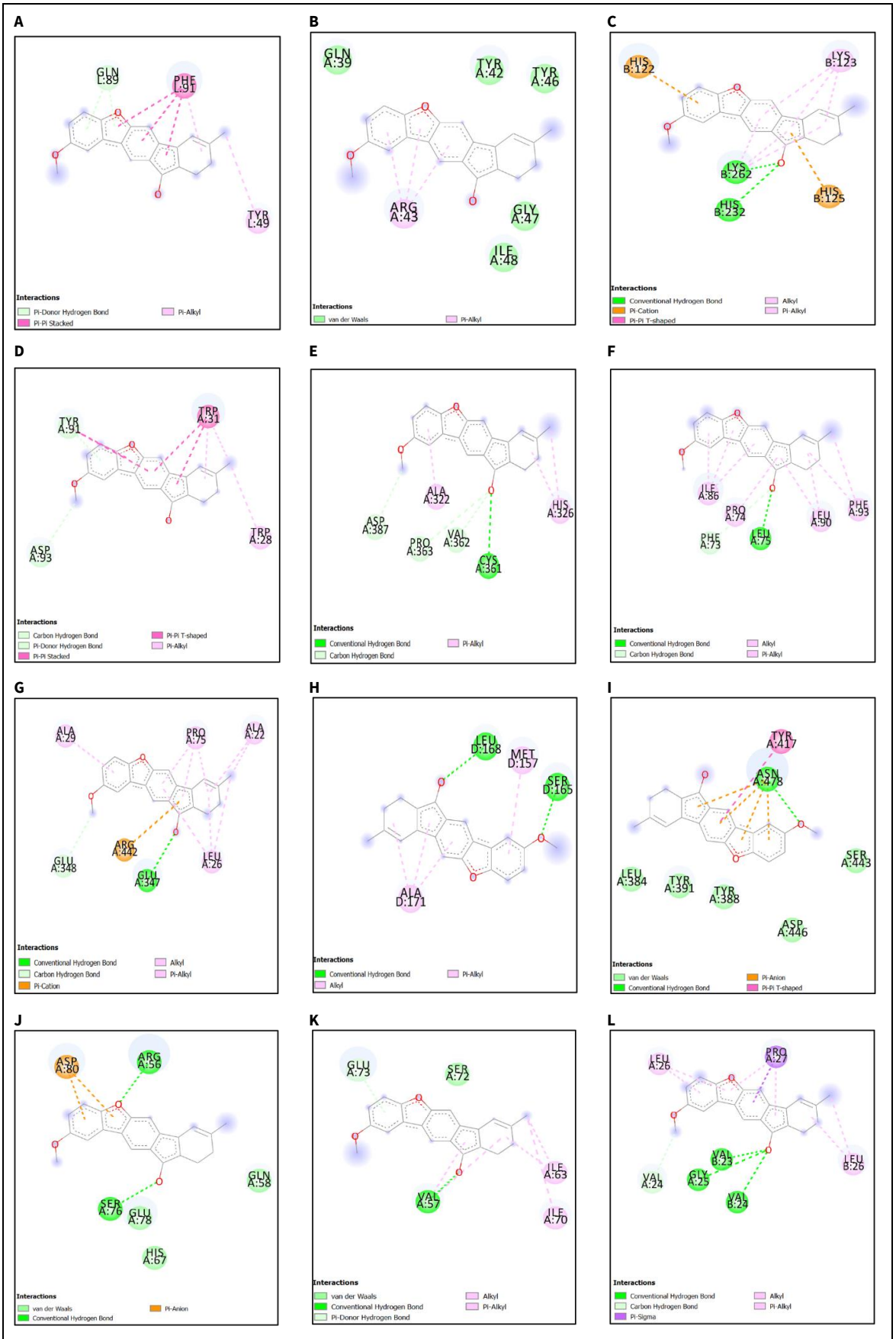

Figure 3. Visualization of two-dimensional chemical interaction.

(A) Osteopontin-SS-HA-PEEK; **(B)** Osteocalcin-SS-HA-PEEK; **(C)** Osteonectin-SS-HA-PEEK; **(D)** BMP4-SS-HA-PEEK; **(E)** BMP2-SS-HA-PEEK; **(F)** BMP7-SS-HA-PEEK; **(G)** ALP-SS-HA-PEEK; **(H)** RUNX2-SS-HA-PEEK; **(I)** IGF1-SS-HA-PEEK; **(J)** Osterix-SS-HA-PEEK; **(K)** TRAPase-SS-HA-PEEK; **(L)** COL1A1-SS-HA-PEEK.

Table 5. Network assessment of ligand candidates.

Protein name	Ligand	Network analysis			
		Average number of neighbors	Number of nodes	Number of edges	Characteristic path length
Osteopontin/SPP1	SS-HA-PEEK	10.381	21	109	1.481
Osteocalcin/BGLAP	SS-HA-PEEK	9.238	21	97	1.538
Osteonectin/SPARC	SS-HA-PEEK	9.429	21	99	1.529
BMP4	SS-HA-PEEK	15.429	21	162	1.229
BMP2	SS-HA-PEEK	17.048	21	179	1.148
BMP7	SS-HA-PEEK	16.900	20	169	1.111
AP/ALPL	SS-HA-PEEK	6.857	21	72	1.657
RUNX2	SS-HA-PEEK	11.810	21	124	1.410
IGF1	SS-HA-PEEK	11.905	21	125	1.405
Osterix/SP7	SS-HA-PEEK	12.842	19	122	1.287
TRAPase/ACP5	SS-HA-PEEK	10.400	20	104	1.453
COL1A1	SS-HA-PEEK	14.857	21	156	1.257

Binding sites are made up of different kinds of amino acid residues that interact with ligand atoms; these residues serve as interaction hotspots (Montelone et al., 2022).

Ligand activity on the target proteins can be triggered by hydrogen, van der Waals, electrostatic, hydrophobic, pi, and alkyl chemical bonds that were created in contact hotspots. The hydrogen, van der Waals, pi, and alkyl bonds that were formed in this investigation could cause ligand action on the target proteins (Yazdani et al., 2023). These weak bonds contributed to specificity and affinity and were necessary for the stability of bond interactions in ligand-protein complexes (Torres et al., 2019). To ensure stability, there must be fewer than three unfavorable bond interactions that cause ligand-protein complexes to become unstable (Kemmish et al., 2017).

Pathway prediction aims to understand biological systems, discover how important proteins function in determining possible targets, evaluate omics data, and comprehend how to integrate target pathway-related information from scientific literature and some experimental data. The accuracy of network prediction is significantly influenced by the information gathered via route prediction, which includes the typical path length, the average number of neighbors, and the number of nodes and edges (Franz et al., 2023). The average value of the link between nodes and edges in the network is represented by the average number of neighbors. To suggest a high likelihood of ligand activity influencing biological responses along the route, the average number of neighbors must be greater than zero (Koutrouli et al., 2020). The network's capacity to transmit activity information, including activators and inhibitors, is represented by the typical path length value; values less than two imply a quicker network (Mousavian et al., 2021).

According to this study's findings, the SS + PEEK + HA complex suppressed TRAPase but increased activity when bound to osteopontin, osteocalcin, osteonectin, BMP4, BMP2, BMP7, ALP, RUNX2, IGF1, osterix, and COL1A1. The recruitment, proliferation, and differentiation of osteoprogenitor cells into mature osteoblasts, followed by the generation of extracellular matrix and mineralization at the surface, were necessary for the development of mineralized bone at the bone-implant contact. *In vitro*, osteoblast maturation occurred in three primary developmental phases: growth and proliferation, extracellular matrix formation and maturation, and mineralization. Each stage was characterized by distinct alterations in gene expression (Wennerberg et al., 2015).

RUNX2, osterix, COL1A1, BMP2, BMP4, and BMP7 were markers of early osteogenic development. Advanced osteogenic indicators included osteocalcin and osteopontin (Gromolak et al., 2020). An essential signaling mechanism for osteogenesis was BMP. The intracellular protein fusion of *Caenorhabditis elegans* Sma genes and the *Drosophila* Mad, Mothers against decapentaplegic (SMAD), which regulates the production of the master gene RUNX2, was first activated by the BMP pathway (Valenti et al., 2017). Mesenchymal stem cells, which are multipotent cells with the ability to develop along many cell lineages, were the primary source of osteoprogenitor cells.

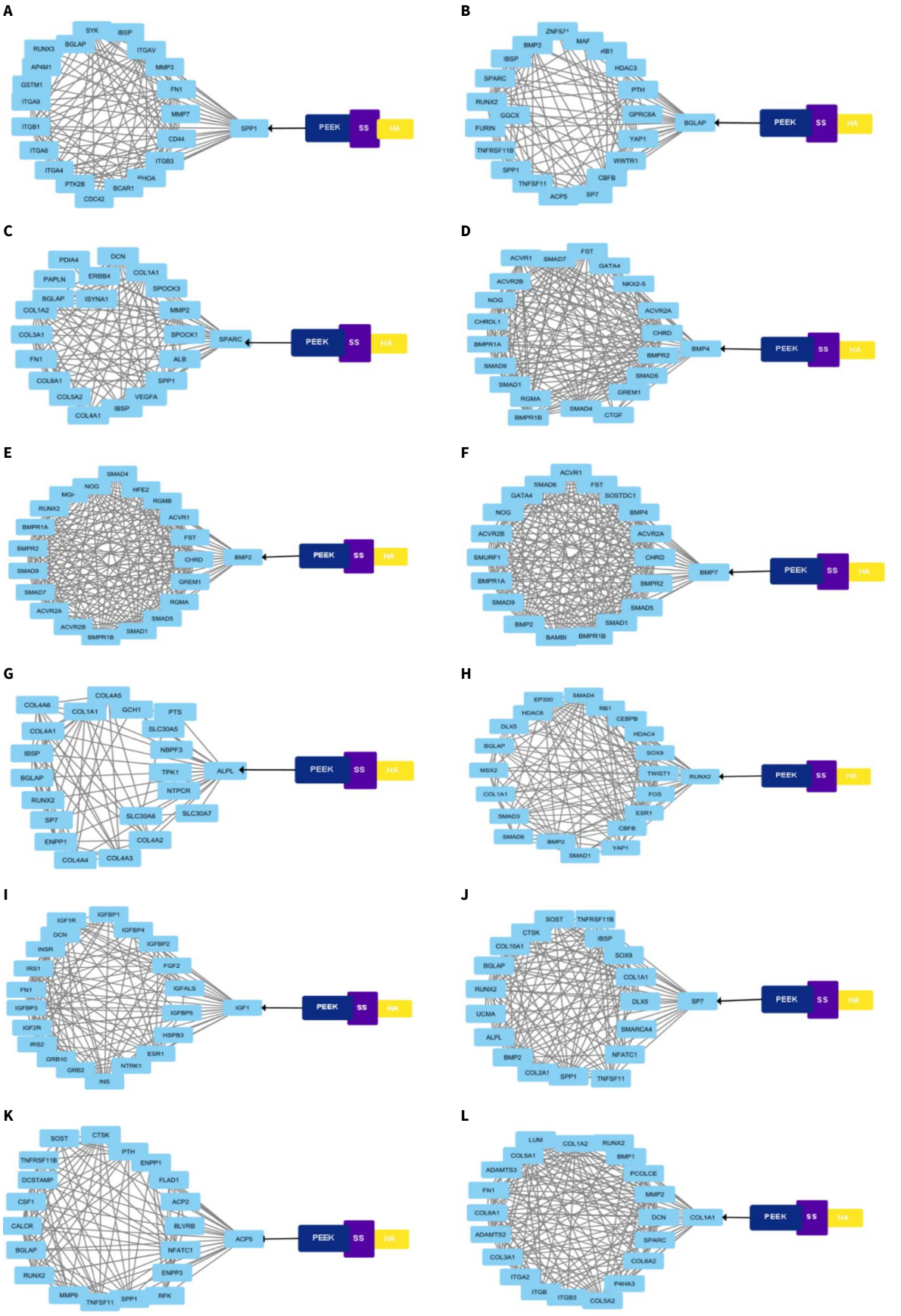

Figure 4. Biological network of SS-HA-PEEK interaction with the whole target through circular mode.

T-shapes indicate inhibition, and arrows represent activation. **(A)** Osteopontin-SS-HA-PEEK; **(B)** Osteocalcin-SS-HA-PEEK; **(C)** Osteonectin-SS-HA-PEEK; **(D)** BMP4-SS-HA-PEEK; **(E)** BMP2-SS-HA-PEEK; **(F)** BMP7-SS-HA-PEEK; **(G)** ALP-SS-HA-PEEK; **(H)** RUNX2-SS-HA-PEEK; **(I)** IGF1-SS-HA-PEEK; **(J)** Osterix-SS-HA-PEEK; **(K)** TRAPase-SS-HA-PEEK; **(L)** COL1A1-SS-HA-PEEK.

During bone formation, RUNX2 was an essential transcription factor for osteoblast differentiation, matrix synthesis, and mineralization. Furthermore, osterix was regulated by RUNX2 (Nugraha et al., 2019; Sitasari et al., 2020). Osteoblasts express the zinc-finger transcription factor osterix, which is crucial for bone production and osteoblast differentiation. Since ALP was an early indicator of osteoblast differentiation and helped make the extracellular matrix competent for mineralization, its expression rose during extracellular matrix maturation and fell when mineralization was fully developed (Megat Badarul Hisham et al., 2019). Additionally, RUNX2 controlled important downstream genes unique to osteoblasts, including COL1A1, osteopontin, and osteocalcin, which were translated into matrix proteins and dictated osteoblast phenotype and function in skeletogenesis. To put it another way, osterix, which was regulated by RUNX2, affected COL1A1, osteopontin, and osteocalcin (Choi et al., 2017). Type I collagen (COL1) was expressed in large quantities during the early synthesis stage of osteoblast differentiation, promoting cell proliferation. As cells matured, their expression progressively declined. With the beginning of osteoblast development, bone sialoprotein was momentarily expressed; with the beginning of mineralization, it increased once more in differentiated osteoblasts. Early in bone cell development, osteopontin, a sialoprotein that facilitated HA binding, was generated; once mineralization started, its expression levels increased. Only completely developed osteoblasts expressed osteocalcin, which was evident during mineralization (Wennerberg et al., 2015).

CONCLUSION

Molecular docking studies indicated that the combination of SS, PEEK, and nano-HA holds great potential as a material for OMI. SS, PEEK, and HA ligands had a high binding affinity for resistance-form-related bone target proteins, such as osteopontin and IGF1. High binding ability and behaviors, including inhibition and activation, were exhibited by ligands with greater negative binding affinity values. More research is required *in vitro*, *in vivo*, and in clinical study settings to examine the mechanical, biological, and chemical characteristics of SS, PEEK, and nano-HA combinations.

CONFLICT OF INTEREST

The authors declare no conflicts of interest.

ACKNOWLEDGMENTS

Authors thank Faculty of Dental Medicine, Universitas Airlangga and Faculty of Dentistry, Universiti Sains Malaysia for supporting our study. This study was supported by International Research Collaboration 300th funded by Universitas Airlangga, Indonesia 2024 fiscal year.

REFERENCES

Alenezi A, Galli S, Atefyekta S, Andersson M, Wennerberg A (2019) Osseointegration effects of local release of strontium ranelate from implant surfaces in rats. J Mater Sci Mater Med 30(10): 116. https://doi.org/10.1007/s10856-019-6314-y

Alhammadi MS, Halboub E, Fayed MS, Labib A, El-Saaidi C (2023) Global distribution of malocclusion traits: A systematic review. DentPress J Orthod 23(6): 40.e1. https://doi.org/10.1590/2177-6709.23.6.40.e1-10.onl

Ardani IGAW, Hariati IVD, Nugraha AP, Narmada IB, Syaifudin A, Perkasa IBA (2024) Comparison of biomechanical performance of titanium and polyaryletheretherketone miniscrews at different insertion angles: A finite element analysis. J Ortho Sci 31: 13. https://doi.org/10.4103/jos.jos_102_23

Ardani IG, Nugraha AP, Suryani MN, Pamungkas RH, Vitamamy DG, Susanto RA, Sarno R, Fajar A, Kharisma VD, Putera A (2022) Molecular docking of polyether ether ketone and nano-hydroxyapatite as biomaterial candidates for orthodontic mini-implant fabrication. J Pharm Pharmacogn Res 10(4): 676–686. https://doi.org/10.56499/jppres22.1371_10.4.676

Ardani IGAW, Nugraha AP, Vitamamy DG, Gautama S, Alida, Rahmawati D (2023) Correlation of malocclusion with facial profile in Javanese population: A cephalometric analysis. J Int Dent Medical Res 16(2): 756–765.

Ardani IG, Rahmawati D, Narmada IB, Nugraha AP, Taftazani H, Kusumawardani MK (2020) Surface electromyography unveil the relationship between masticatory muscle tone and maloclusion class I & II in Javanese ethnic patient. J Int Dent Medical Res 13(4): 1447–1454.

Berniyanti T, Nugraha AP, Hidayati NN, Kharisma VD, Nugraha AP, Noor TNEBTA (2022) Computational study of Cu^{2+}, Fe^{2+}, Mn^{2+}, Mn^{3+}, Fe^{3+}, CrO_4^{2-}, Si^{4+}, and Hg^{+} binding sites identification on cytokines to predict dental metal allergy: An *in silico* study. J Pharm Pharmacogn Res 10(4): 687–694. https://doi.org/10.56499/jppres22.1372_10.4.687

Botelho FD, dos Santos MC, Gonçalves A da S, Kuca K, Valis M, LaPlante SR, França TC, de Almeida JS (2020) Ligand-based virtual screening, molecular docking, molecular dynamics, and MM-PBSA calculations towards the identification of potential novel ricin inhibitors. Toxins 12(12): 746. https://doi.org/10.3390/toxins12120746

Bueno J (2020) ADMETox: Bringing Nanotechnology Closer to Lipinski's Rule of Five. In: Preclinical Evaluation of Antimicrobial Nanodrugs. Nanotechnology in the Life Sciences. Springer, Cham. https://doi.org/10.1007/978-3-030-43855-5_5

Byeon SM, Kim HJ, Lee MH, Bae TS (2022) Enhancement of bioactivity and osseointegration in Ti-6Al-4V orthodontic mini-screws coated with calcium phosphate on the TiO_2 nanotube layer. Korean J Orthod 52(6): 412–419. https://doi.org/10.4041/kjod22.118

Cecilia PH, Nugraha AP, Shariff KA, Kharisma VD, Ramadhani NF, Sitalaksmi RM (2024) Molecular docking of beta tricalcium phosphate combined with dicalcium phosphate

dihydrate compared to hydroxyapatite induced osteogenesis biomarker: A bioinformatic approach. J Int Dent Medical Res 17(2): 470–479.

Cheng Z, Guo C, Dong W, He FM, Zhao SF, Yang GL (2012) Effect of thin nano-hydroxyapatite coating on implant osseointegration in ovariectomized rats. Oral Surg Oral Med Oral Pathol Oral Radiol. 113(3): e48-53. https://doi.org/10.1016/j.tripleo.2011.07.008

Choi JW, Shin S, Lee CY, Lee J, Seo HH, Lim S, Lee S, Kim IK, Lee HB, Kim SW, Hwang KC (2017) Rapid induction of osteogenic markers in mesenchymal stem cells by adipose-derived stromal vascular fraction cells. Cell Phy Biochem 44(1): 53–65. https://doi.org/10.1159/000484582

Daina A, Michielin O, Zoete V (2019) Swiss Target Prediction: updated data and new features for efficient prediction of protein targets of small molecules. Nucleic Acids Res 47(W1): W357–W364. https://doi.org/10.1093/nar/gkz382

Delicia D, Amalia NR, Nugraha AP, Pramusita A, Kharisma VD, Narmada IB (2024) A bioinformatic approach of stingless bee's (*Trigona biroi*) propolis active constituent for antioxidant, growth factor and osteoblastogenesis molecular pathway prediction. J Int Dent Med Res 17(2): 591–602.

Ertan-Bolelli T, Bolelli K (2021) *In silico* design of novel sirtuin 1 enzyme activators for the treatment of age-related diseases and life span. Curr Comput Aided Drug Des 17(3): 412–420. https://doi.org/10.2174/1573409916666200422074441

Franz M, Lopes CT, Fong D, Kucera M, Cheung M, Siper MC, Huck G, Dong Y, Sumer O, Bader GD (2023) Cytoscape.js 2023 update: A graph theory library for visualization and analysis. Bioinformatics *39*(1): btad031. https://doi.org/10.1093/bioinformatics/btad031

García-Ortegón M, Simm GNC, Tripp AJ, Hernández-Lobato JM, Bender A, Bacallado S (2022) DOCKSTRING: Easy molecular docking yields better benchmarks for ligand design. J Chem Inf Model 62(15): 3486–3502. https://doi.org/10.1021/acs.jcim.1c01334

Gkantidis N, Christou P, Topouzelis N (2010) The orthodontic–periodontic interrelationship in integrated treatment challenges: A systematic review. J Oral Rehabil 37(5): 377–390. https://doi.org/10.1111/j.1365-2842.2010.02068.x

Gromolak S, Krawczenko A, Antończyk A, Buczak K, Kiełbowicz Z, Klimczak A (2020) Biological characteristics and Osteogenic Differentiation of Ovine Bone Marrow Derived Mesenchymal Stem Cells Stimulated with FGF-2 and BMP-2. Int J Mol Sci 21(24): 9726. https://doi.org/10.3390/ijms21249726

Hata H, Phuoc Tran D, Marzouk Sobeh M, Kitao A (2021) Binding free energy of protein/ligand complexes calculated using dissociation parallel cascade selection molecular dynamics and Markov state model. Biophys Physicobiol 18: bppb-v18.037. https://doi.org/10.2142/biophysico.bppb-v18.037

Ivanova L, Karelson M (2022) The impact of software used and the type of target protein on molecular docking accuracy. Molecules 27(24): 9041. https://doi.org/10.3390/molecules27249041

Karakoti H, Mahawer SK, Tewari M, Kumar R, Prakash O, de Oliveira MS, Rawat DS (2022) Phytochemical profile, *in vitro* bioactivity evaluation, *in silico* molecular docking and ADMET study of essential oils of three *Vitex* species grown in Tarai Region of Uttarakhand. Antioxidants 11(10): 1911. https://doi.org/10.3390/antiox11101911

Kayhan ZO, Kazazoğlu E (2018) An overview of implant stability measurement. modern approaches in dentistry and oral health care. Mod App Dent Oral Health 2(5): 212–215. https://doi.org/10.32474/MADOHC.2018.02.000149

Kemmish H, Fasnacht M, Yan L (2017) Fully automated antibody structure prediction using BIOVIA tools: Validation study. PLoS One 12(5): e0177923. https://doi.org/10.1371/journal.pone.0177923

Kharisma VD, Ansori ANM, Dian FA, Rizky WC, Dings TGA, Zainul R, Nugraha AP (2021a) Molecular docking and dynamic simulation of entry inhibitor from *Tamarindus indica* bioactive compounds against SARS-Cov-2 infection via viroinformatics study. Biochem Cell Arch 21(2): 3323–3327.

Kharisma VD, Ansori ANM, Widyananda MH, Utami SL, Nugraha AP (2020) Molecular simulation: The potency of conserved region on E6 HPV-16 as a binding target of black tea compounds against cervical cancer. Biochem Cell Arch 20:2795-2802.

Kharisma VD, Widyananda MH, Ansori ANM, Nege AS, Naw SW, Nugraha AP (2021b) Tea catechin as antiviral agent via apoptosis agonist and triple inhibitor mechanism against HIV-1 infection: A bioinformatics approach. J Pharm Pharmacogn Res 9(4): 435–445. https://doi.org/10.56499/jppres21.1009_9.4.435

Khotib J, Lasandara CS, Samirah S, Budiatin AS (2019) Acceleration of bone fracture healing through the use of natural bovine hydroxyapatite implant on bone defect animal model. Folia Med Indonesiana 55(3): 176–187. https://doi.org/10.20473/fmi.v55i3.15495

Kim S (2016) Getting the most out of PubChem for virtual screening. Expert Opin Drug Discov 11(9): 843–855. https://doi.org/10.1080/17460441.2016.1216967

Konc J, Janežič D (2022) Protein binding sites for drug design. Biophys Rev 14(6): 1413–1421. https://doi.org/10.1007/s12551-022-01028-3

Koutrouli M, Karatzas E, Paez-Espino D, Pavlopoulos GA (2020) A guide to conquer the biological network era using graph theory. Front Bioeng Biotechnol 8: 34. https://doi.org/10.3389/fbioe.2020.00034

Leo M, Cerroni L, Pasquantonio G, Condò SG, Condò R (2016) Temporary anchorage devices (TADs) in orthodontics: Review of the factors that influence the clinical success rate of the mini-implants. Clin Ter 167(3): e70-77. https://doi.org/10.7417/CT.2016.1936

Levingstone TJ, Ardhaoui M, Benyounis K, Looney L, Stokes JT (2015) Plasma sprayed hydroxyapatite coatings: Understanding process relationships using design of experiment analysis. Surf Coat Technol 283: 29–36. https://doi.org/10.1016/j.surfcoat.2015.10.044

Listiyani P, Kharisma VD, Ansori AN, Widyananda MH, Probojati RT, Murtadlo AA, Turista DD, Ullah ME, Jakhmola V, Zainul R (2022) *In silico* phytochemical compounds screening of *Allium sativum* targeting the Mpro of SARS-CoV-2. Pharmacogn J 14(3): 604–609. https://doi.org/10.5530/pj.2022.14.78

Ma Z, Zhao X, Zhao J, Zhao Z, Wang Q, Zhang C (2020) Biologically modified polyether ether ketone as dental implant material. Front Bioeng Biotechnol 8: 620537. https://doi.org/10.3389/fbioe.2020.620537

Makar LE, Nady N, Shawky N, Kandil SH (2023) Genipin versus ferric chloride cross-linked unmodified Gum Arabic/Chitosan/nano-Hydroxyapatite nanocomposite hydrogels as potential scaffolds for bone regeneration. Sci Rep 13(1): 14402. https://doi.org/10.1038/s41598-023-41413-w

Megat Badarul Hisham PN, Narmada I, Alida A, Rahmawati D, Nugraha A, Putranti N (2019) Effects of vitamin D in alveolar bone remodeling on osteoblast numbers and bone alkaline phosphatase expression in pregnant rats during orthodontic tooth movement. J Orofac Sci 11(2): 79–83. https://doi.org/10.4103/jofs.jofs_10_19

Monteleone S, Fedorov DG, Townsend-Nicholson A, Southey M, Bodkin M, Heifetz A (2022) Hotspot identification and drug

design of protein-protein interaction modulators using the fragment molecular orbital method. J Chem Inf Model 62(16): 3784–3799. https://doi.org/10.1021/acs.jcim.2c00457

Mousavian Z, Khodabandeh M, Sharifi-Zarchi A, Nadafian A, Mahmoudi A (2021) StrongestPath: A Cytoscape application for protein–protein interaction analysis. BMC Bioinformatics 22(1): 352. https://doi.org/10.1186/s12859-021-04230-4

Naini A, Sudiana IK, Rubianto M, Kresnoadi U, Latief FDE (2019) Effects of hydroxyapatite gypsum puger scaffold applied to rat alveolar bone sockets on osteoclasts, osteoblasts and the trabecular bone area. Dent J 52(1): 13–17. https://doi.org/10.20473/j.djmkg.v52.i1.p13-17

Najeeb S, Bds ZK, Bds SZ, Bds MS (2016) Bioactivity and osseointegration of PEEK are inferior to those of titanium: A systematic review. J of Oral Implant 42(6): 512–516. https://doi.org/10.1563/aaid-joi-D-16-00072

Neto JVC, Teixeira ABV, Cândido Dos Reis A (2023) Hydroxyapatite coatings versus osseointegration in dental implants: A systematic review. J Prosthet Dent S0022-3913(23): 00631–5. https://doi.org/10.1016/j.prosdent.2023.09.019

Nugraha AP, Narmada IB, Ernawati DS, Dinaryanti A, Hendrianto E, Ihsan IS, Riawan W, Rantam FA (2019) The aggrecan expression post platelet rich fibrin administration in gingival medicinal signaling cells in Wistar rats (*Rattus novergicus*) during the early osteogenic differentiation (*in vitro*). Kafkas Univ Vet Fak Derg 25(3): 421–425. https://doi.org/10.9775/kvfd.2018.21174

Nugraha AP, Sibero MT, Nugraha AP, Puspitaningrum MS, Rizqianti Y, Rahmadhani D, Kharisma VD, Ramadhani NF, Ridwan RD, Noor TNEBTA, Ernawati DS (2023) Anti-periodontopathogenic ability of mangrove leaves (*Aegiceras corniculatum*) ethanol extract: *In silico* and *in vitro* study. Eur J Dent 17(1): 46-56. https://doi.org/10.1055/s-0041-1741374

Park KH, Choi JY, Kim KA, Kim SJ, Chung KR, Kim SH (2021) Critical issues concerning biocreative strategy in contemporary temporary skeletal anchorage device orthodontics: A narrative review. Orthod Craniofac Res 24(S1): 39–47. https://doi.org/10.1111/ocr.12444

Prahasanti C, Nugraha AP, Kharisma VD, Ansori AN, Devijanti R, Ridwan TP, Ramadhani NF, Narmada IB, Ardani IG, Noor TN (2021) A bioinformatic approach of hydroxyapatite and polymethylmethacrylate composite exploration as dental implant biomaterial. J Pharm Pharmacogn Res 9(5): 746–54. http://dx.doi.org/10.56499/jppres21.1078_9.5.746

Putri VAV, Triwardhani A, Noor TNEBTA, Nugraha AP (2024) Orthodontic treatment needs and malocclusion prevalence according to index of complexity, outcome and need in Kediri, Indonesian 7- to -13 years-old children. J Int Dent Med Res 17(2): 764–768.

Ramadhani NF, Nugraha AP, Rahmadani D, Puspitaningrum MS, Rizqianti Y, Kharisma VD, Noor TNEBTA, Ridwan RD, Ernawati DS, Nugraha AP (2022) Anthocyanin, tartaric acid, ascorbic acid of roselle flower (*Hibiscus sabdariffa* L.) for immunomodulatory adjuvant therapy in oral manifestation coronavirus disease-19: An immunoinformatic approach. J Pharm Pharmacogn Res 10(3): 418–428. https://doi.org/10.56499/jppres21.1316_10.3.418

Rose PW, Prlić A, Altunkaya A, Bi C, Bradley AR, Christie CH, Costanzo LD, Duarte JM, Dutta S, Feng Z, Green RK (2017) The RCSB protein data bank: Integrative view of protein, gene and 3D structural information. Nucleic Acids Res 45(D1): D271–D281. https://doi.org/10.1093/nar/gkw1000

Saskianti T, Nugraha AP, Prahasanti C, Ernawati DS, Tanimoto K, Riawan W, Kanawa M, Kawamoto T, Fujimoto K (2022) Study of Alveolar bone remodeling using deciduous tooth stem cells and hydroxyapatite by vascular endothelial growth factor enhancement and inhibition of matrix metalloproteinase-8 expression *in vivo*. Clin Cosmet Investig Dent 14: 71–78. https://doi.org/10.2147/CCIDE.S354153

Shallangwa GA, Adeniji SE (2021) Binding profile of protein-ligand inhibitor complex and structure-based design of new potent compounds via computer-aided virtual screening. J Clin Tuberc Other Mycobact Dis 24: 100256. https://doi.org/10.1016/j.jctube.2021.100256

Sitasari PI, Narmada IB, Hamid T, Triwardhani A, Nugraha AP, Rahmawati D (2020) East Java green tea methanolic extract can enhance RUNX2 and osterixexpression during orthodontic tooth movement *in vivo*. J Pharm Pharmacogn Res 8(4): 290–298. http://dx.doi.org/10.56499/jppres19.787_8.4.290

Syahdinda MR, Nugraha AP, Triwardhani A, Noor TNEBTA (2022) Management of impacted maxillary canine with surgical exposure and alignment by orthodontic treatment. Dent J 55(4): 235–239. https://doi.org/10.20473/j.djmkg.v55.i4.p235-239

Torres PHM, Sodero ACR, Jofily P, Silva-Jr FP (2019) Key topics in molecular docking for drug design. Int J Mol Sci 20(18): 4574. https://doi.org/10.3390/ijms20184574

Tošović J, Fijan D, Jukič M, Bren U (2022) Conserved water networks identification for drug design using density clustering approaches on positional and orientational data. J Chem Inf Model 62(23): 6105–6117. https://doi.org/10.1021/acs.jcim.2c00801

Valenti MT, Carbonare LD, Mottes M (2017) Osteogenic differentiation in healthy and pathological conditions. Int J Mol Sci 18(1): 41. https://doi.org/10.3390/ijms18010041

Wennerberg A, Jimbo R, Albrektsson T (2015) Implant surfaces and their biological and clinical impact. Implant Surfaces and their Biological and Clinical Impact. Heidelberg: Springer Berlin, pp. 1–182. https://doi.org/10.1007/978-3-662-45379-7

Yazdani M, Jafari A, Mahdian S, Namazi M, Gharaghani S (2023) Rational approaches to discover SARS-CoV-2/ACE2 interaction inhibitors: Pharmacophore-based virtual screening, molecular docking, molecular dynamics and binding free energy studies. J Mol Liq 375: 121345. https://doi.org/10.1016/j.molliq.2023.121345

Yusuf A, Almotairy ARZ, Henidi H, Alshehri OY, Aldughaim MS (2023) Nanoparticles as drug delivery systems: A review of the implication of nanoparticles' physicochemical properties on responses in biological systems. Polymers (Basel) 15(7): 1596. https://doi.org/10.3390/polym15071596

AUTHOR CONTRIBUTION:

Contribution	Ardani IGAW	Sugitto MR	Aufa HR	Kharisma VD	Putranto AF	Gunung GP	Perkasa IBA	Syaifudin A	Situmorang PC	Hassan R	Nugraha AP
Concepts or ideas	x							x	x	x	x
Design	x			x				x	x	x	x
Definition of intellectual content	x			x						x	x
Literature search	x	x	x							x	x
Experimental studies	x	x	x	x				x			x
Data acquisition	x	x	x	x				x			x
Data analysis	x	x	x	x				x			x
Statistical analysis	x	x	x	x				x			x
Manuscript preparation	x	x	x		x	x	x	x	x	x	x
Manuscript editing	x	x	x		x	x	x	x	x	x	x
Manuscript review	x	x	x	x	x	x	x	x	x		

Citation Format: Ardani IGAW, Sugitto MR, Aufa HR, Kharisma VD, Putranto AF, Gunung GP, Perkasa IBA, Syaifudin A, Situmorang PC, Hassan R, Nugraha AP (2025) Hydroxyapatite, polyetheretherketone, and stainless steel as orthodontic mini-implant biomaterial candidates: A bioinformatic approach. J Pharm Pharmacogn Res 13(3): 801–815. https://doi.org/10.56499/jppres24.2049_13.3.801

Publisher's Note: All claims expressed in this article are solely those of the authors and do not necessarily represent those of their affiliated organizations, or those of the publisher, the editors and the reviewers. Any product that may be evaluated in this article, or claim that may be made by its manufacturer, is not guaranteed or endorsed by the publisher.

Open Access: This article is distributed under the terms of the Creative Commons Attribution 4.0 International License (http://creativecommons.org/ licenses/by/4.0/), which permits use, duplication, adaptation, distribution and reproduction in any medium or format, as long as you give appropriate credit to the original author(s) and the source, provide a link to the Creative Commons license and indicate if changes were made.